American Journal of Pathology, Vol. 160, No. 3, March 2002

Fibrinogen Stabilizes Placental-Maternal Attachment During Embryonic Development in the Mouse

Takayuki Iwaki, Mayra J. Sandoval-Cooper, Melissa Paiva, Takao Kobayashi, Victoria A. Ploplis, and Francis J. Castellino

From the W. M. Keck Center for Transgene Research and the Department of Chemistry and Biochemistry, University of Notre Dame, Notre Dame, Indiana

In humans, maternal fibrinogen (Fg) is required to support pregnancies by maintaining hemostatic balance and stabilizing uteroplacental attachment at the fibrinoid layer found at the fetal-maternal junction. To examine relationships between low Fg levels and early fetal loss, a genetic model of afibrinogenemia was developed. Pregnant mice homozygous for a deletion of the Fg-γ chain, which results in a total Fg deficiency state ($FG^{-/-}$), aborted the fetuses at the equivalent gestational stage seen in humans. Results obtained from timed matings of $FG^{-/-}$ mice showed that vaginal bleeding was initiated as early as embryonic day (E)6 to 7, a critical stage for maternal-fetal vascular development. The condition of afibrinogenemia retarded embryo-placental development, and consistently led to abortion and maternal death at E9.75. Lack of Fg did not alter the extent or distribution pattern of other putative factors of embryo-placental attachment, including laminin, fibronectin, and Factor XIII, indicating that the presence of fibrin(ogen) is required to confer sufficient stability at the placental-decidual interface. The results of these studies demonstrate that maternal Fg plays a critical role in maintenance of pregnancy in mice, both by supporting proper development of fetal-maternal vascular communication and stabilization of embryo implantation. ***(Am J Pathol 2002, 160:1021–1034)***

Fibrinogen (Fg) is a 340-kd symmetrical heterodimeric protein consisting of three pairs of nonidentical polypeptide chains, and has an overall structure of $(A\alpha/B\beta/\gamma)_2$. This protein is the precursor of fibrin, formed during the hemostatic response. Three separate genes, *FGA*, *FGB*, and *FGG*, located on a 50-kb region of chromosome 4q28-q31, are translated in a coordinated fashion to code for the Aα-, Bβ-, and γ-chains, respectively, of Fg.[1] For its conversion into fibrin, thrombin first catalyzes release of fibrinopeptides A and B from the Aα and Bβ chains, thus leading to exposure of polymerization sites that organize the initially formed fibrin monomers into a polymeric network of fibers that form the major protein component of the blood clot. This clot is ultimately covalently stabilized by crosslinking of specific ϵ-NH_2 groups of Lys and γ-COOH groups of Glu residues of fibrin monomer, a process catalyzed by a transglutaminase, namely, activated Factor XIII (FXIIIa).[2]

In addition to their function in clot formation, Fg and fibrin play roles in other pathophysiological processes, such as infection,[3] wound healing,[4,5] and clot retraction.[6] Further, both Fg and fibrin have been implicated in the progression of certain types of tumors,[7] and in the severity of atherosclerosis.[8]

Congenital afibrinogenemia (MIM no. 202400), an autosomal recessive disorder, was first described in 1920,[9] and since that time more than 150 cases have been reported.[10] The underlying causes of afibrinogenemia have been determined to be because of a large number of genetic abnormalities in *FGA* (donor splice site, frameshift, and nonsense mutations);[11,12] FGB (missense mutations);[13] and *FGG* (deletion, splice site, and missense mutations).[14–16] Despite excessively prolonged plasma clot times, the phenotypes manifested by these patients involve hemorrhagic diatheses no more severe than hemophilia A or B. A common event after birth is an uncontrolled bleeding from the umbilical cord. Later in life, spontaneous intracerebral bleeding and splenic rupture may occur.[17]

Fg deficiencies also result in spontaneous miscarriage in the early gestational period.[18–20] Although reasons for fetal loss in pregnant females homozygous for the *FGG* deletion, which results in a total deficiency of Fg ($FG^{-/-}$), are primarily uncertain, protection against premature bleeding, offered in part by Fg, is most likely involved in allowing pregnancy to advance. It has also been proposed that there is a need for maternal Fg for proper anchoring of the cytotrophoblasts after they invade the

Supported by National Institutes of Health (grants HL-13423 to F. J. C. and HL-63682 to V. A. P.), a grant from the W. M. Keck Foundation (to F. J. C.), by the Kleiderer-Pezold Family Endowed Professorship (to F. J. C.), by a grant from the Leda Sears Medical Trust, as well as through collaboration with the Walther Cancer Foundation.

Accepted for publication December 7, 2001.

Current Address of T. K.: Department of Obstetrics and Gynecology, Hamamatsu University School of Medicine, Hamamatsu, Japan.

Address reprint requests to Francis J. Castellino, W. M. Keck Center for Transgene Research and the Department of Chemistry and Biochemistry, 229 Nieuwland Science Hall, University of Notre Dame, Notre Dame, IN 46556. E-mail: castellino.1@nd.edu.

endometrium. This entire process may additionally involve fibronectin (FN) and FXIIIa.[21] To address issues involved in the maintenance of pregnancy of afibrinogenemic females, and the role of Fg in this process, we have developed a murine model of congenital afibrinogenemia by targeted deletion of the entire *FGG* gene that results in $FG^{-/-}$ state.[22] Embryos removed from timed matings of $FG^{-/-}$ females were then analyzed for localization of these specific proteins during implantation and development of pregnancy, up to the time of formation of the chorioallantoic placenta, at which point spontaneous miscarriage occurs. This article provides a report of these studies.

Materials and Methods

Mice

Mice with a targeted deletion of the entire coding sequence of the *FGG* chain were used.[22] The strain was the F1 offspring of the mating of 129 SvJ and C57BL/6J mice. Either wild-type (*WT*) or $FG^{-/-}$ male mice were bred with female mice heterozygous for the *FGG* deletion ($FG^{+/-}$) to obtain all combinations of genotypes, which were identified as previously described.[22]

For timed matings, Gtrosa-26 male mice that express β-galactosidase (β-Gal), purchased from Jackson Laboratories (Bar Harbor, ME), were paired with either normal *WT* or $FG^{-/-}$ females. This mating strategy allowed the distinction of embryonic from maternal tissue in early placentas.

Timed matings of mice, which were paired in the evenings, were used to obtain embryos at various gestational ages. The noontime after the morning of the observation of the vaginal plug was designated as embryonic day (E) 0.5. At the desired gestational stages, entire uteri were removed surgically from the mouse and fixed in 4% paraformaldehyde in phosphate-buffered saline (PBS) (10 mmol/L phosphate/140 mmol/L NaCl, pH 7.2) for 2 hours. The tissue was then processed for histological examinations. After fixation, individual embryos, along with the uterine walls, were excised.

Housing and surgical procedures involving experimental animals were approved by the Institutional Animal Care and Research Advisory Committee of the University of Notre Dame.

Histochemistry and Immunohistochemistry

Preparation of Embryos

The embryos were embedded in paraffin and sectioned at a thickness of 4 μm. Representative slides were routinely stained with hematoxylin II and eosin Y (H&E) (Richard Allen Scientific, Kalamazoo, MI) for morphological analysis. For immunoperoxidase techniques, all slides were incubated in Peroxo-block (Zymed Laboratories, San Francisco, CA) to inhibit endogenous peroxidase activity, and with avidin- and biotin-blocking solutions (Zymed Laboratories) to eliminate endogenous avidin- or biotin-like substances.

In some cases, whole mount embryos were initially stained for β-Gal expression before sectioning. When this was desired, entire uteri were cross-sectioned between embryos. The embryos were then transferred to 70% ethanol before processing. The tissues were rinsed several times in X-Gal rinse buffer (0.02% Nonidet P-40/0.01% sodium deoxycholate/2 mmol/L $MgCl_2$, in PBS), and stained overnight in X-Gal staining solution (5 mmol/L potassium ferrocyanide/5 mmol/L potassium ferricyanide/1 mg/ml X-Gal, from a 40-mg/ml stock in dimethylformamide) (Research Products International, Mount Prospect, IL). After several rinses in PBS, the tissues were dehydrated in graded alcohols, cleared in xylene, infiltrated and embedded in paraffin at 60°C, and finally serially sectioned at 4 μm. The slides were then used for other histochemical and immunohistochemical analyses.

Anti-Von Willebrand Factor (VWF) and Anti-Laminin Double-Labeling

Slides were incubated with trypsin for antigen unmasking, then blocked with normal rabbit serum and placed in DAKO-EPOS rabbit-anti-human-VWF antibody conjugated to horseradish peroxidase (HRP) (DAKO, Carpinteria, CA). The chromogen 3,3′-diaminobenzidine was used for color development. These same sections were then washed, blocked in normal swine serum, and incubated with a rabbit anti-rat laminin polyclonal antibody (DAKO) solution. This was followed by addition of a swine anti-rabbit biotin $F(ab)_2$-IgG solution (DAKO), and then by a streptavidin-HRP conjugate (Biogenex, San Ramon, CA). SG chromogen (Vector Laboratories, Burlingame, CA) was applied for color development. Sections were counterstained with Nuclear Fast Red (Vector Laboratories).

Anti-Fibronectin (FN) Immunostaining

Heat-induced antigen retrieval was accomplished with 0.1 mol/L citrate buffer, pH 6.0. Sections were then blocked with normal swine serum, followed by incubation with a rabbit anti-human FN polyclonal antibody (Labvision, Fremont, CA). Next, swine-anti-rabbit biotin IgG-$F(ab)_2$ complex (DAKO) and streptavidin-HRP conjugate solutions were added in succession. SG chromogen, along with a Nuclear Fast Red counterstain, or, 3-amino-9-ethylcarbazole (AEC), followed with a hematoxylin counterstain (Biomeda, Foster City, CA), were used.

Anti-Fibrin(ogen) Immunostaining

After heat-induced antigen retrieval, as above, a preimmune rabbit serum block was applied. The sections were then incubated in a goat anti-mouse fibrin(ogen) antibody (Nordic Immunology, Tillburg, The Netherlands), followed by rabbit anti-goat IgG in 10% normal mouse serum. A complex of HRP, conjugated to a goat

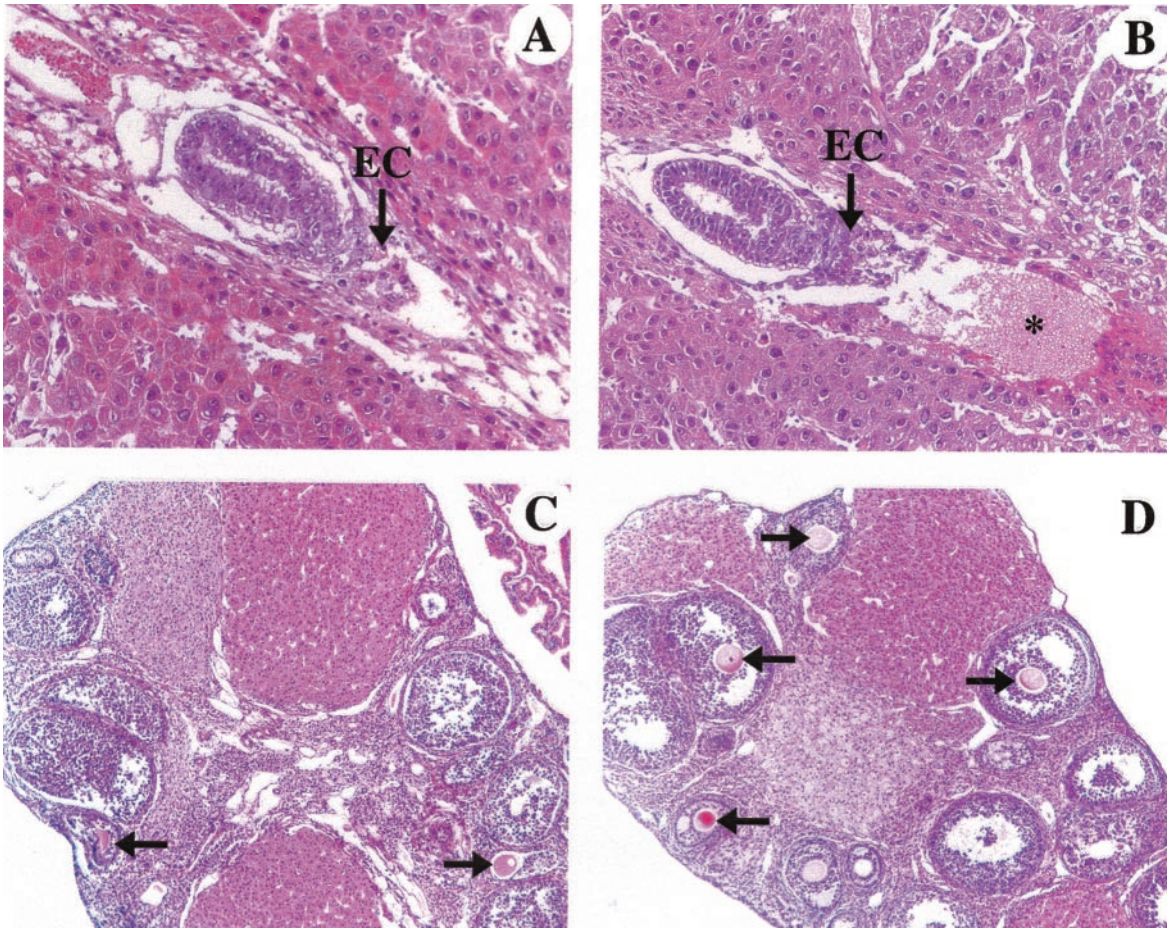

Figure 1. Murine E6.0 uterus and ovaries (original magnifications, ×100). Morphological characterization (H&E staining) of the uteri and ovaries of *WT* and Fg-deficient ($FG^{-/-}$) mice on day 6 of pregnancy (E6). In both *WT* (**A**) and $FG^{-/-}$ (**B**) pregnant mice, implanted embryos appear normal. In both embryos, the ectoplacental cone (EC) seems to be at the same developmental stage. Maternal bleeding (**asterisk**) is seen at the implantation site in the uterus of the $FG^{-/-}$ mouse (**B**). In ovaries of both genotypes (**C** and **D**), evidence of luteinization and intact corpus luteum is seen, along with healthy follicles containing ova (**arrows**).

anti-HRP-IgG solution (DAKO) was added. The slides were developed with AEC and followed with a hematoxylin counterstain.

Anti-FXIII Immunostaining

Heat-induced antigen retrieval was performed on representative slides, as above, followed by a block with normal swine serum. Sections were incubated with a rabbit anti-human FXIII subunit A-polyclonal antibody (Biogenex), followed in succession by biotinylated swine anti-rabbit IgG-F(ab)$_2$ and streptavidin-HRP solutions. AEC chromogen was used for color development. Sections were counterstained with hematoxylin.

Rescue of Pregnancies of $FG^{-/-}$ Female Mice by Fg Supplementation

$FG^{-/-}$ males were paired with $FG^{-/-}$ females and times of vaginal plugs noted. At various times after plug formation, 10 mg of human Fg (Enzyme Research Laboratories, South Bend, IN), dissolved in 0.25 ml of isotonic saline, was administered into the tail veins of the pregnant dams. A volume of 0.1 ml of blood was periodically removed from the eyes of the pregnant females in heparinized capillary tubes, and used for determinations of plasma levels of Fg, using the Fibri-Prest Automate Kit (Diagnostica Stago, Asnieres-Sur-Seine, France).

Results

Based on observations of the courses of numerous pregnancies with $FG^{-/-}$ female mice, it was noted that these mice would consistently present with various degrees of genital bleeding beginning at E7, and undergo spontaneous abortion around E10, with resulting loss of the mother through excessive bleeding. This same phenotype was also reported in another study using mice with a different strategy of generating a $FG^{-/-}$ state.[23] Because this condition also occurs in humans at an equivalent gestational stage, we decided to explore the mechanisms of this effect through a histological examination of murine embryos from normal and $FG^{-/-}$ pregnant females obtained from timed matings from E6 to E9.75.

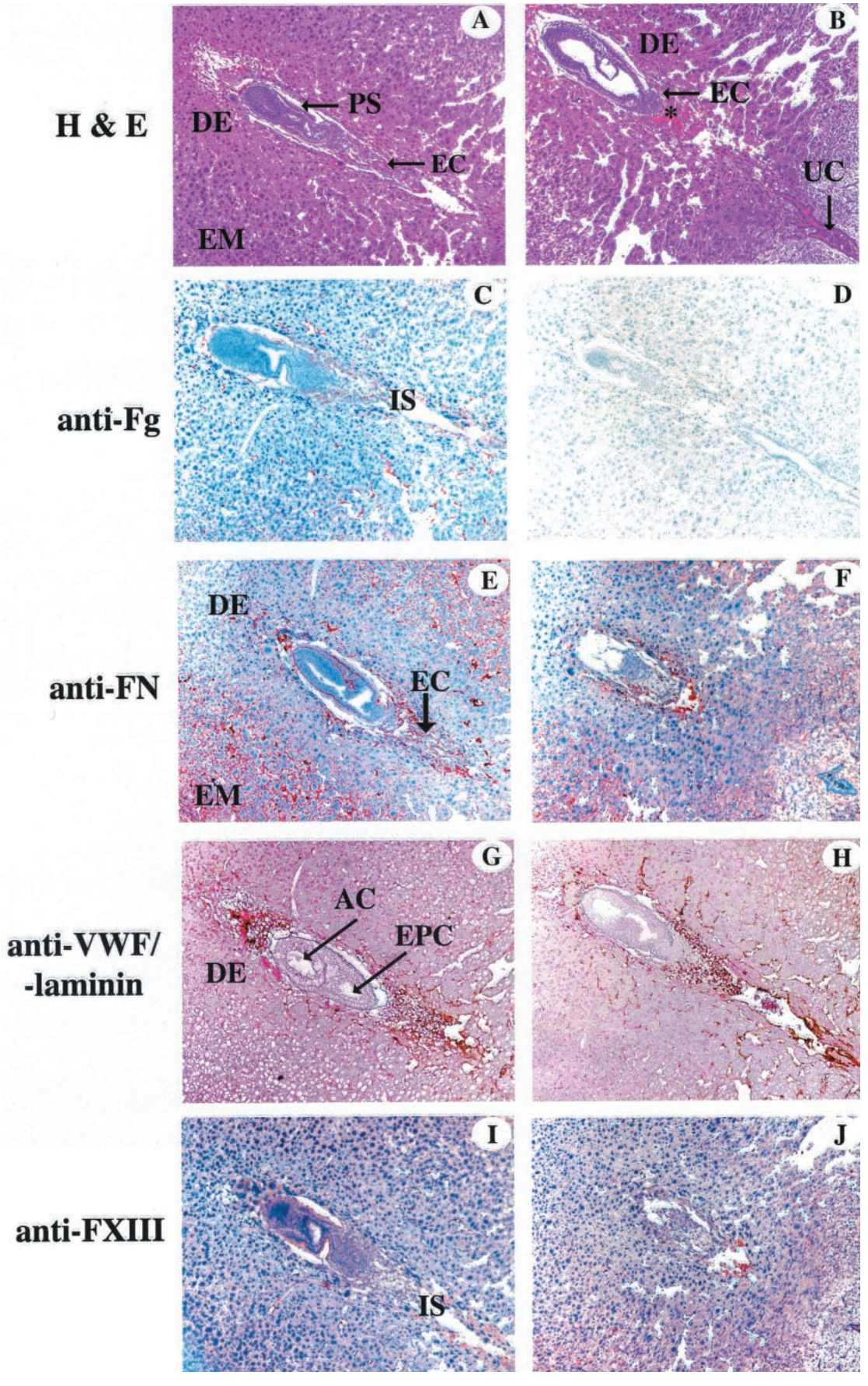
H & E
A
DE
PS
EC
EM
B
DE
EC
*
UC
anti-Fg
C
IS
D
anti-FN
E
DE
EC
EM
F
anti-VWF/
-laminin
G
AC
EPC
DE
H
anti-FXIII
I
IS
J

Histochemical and Immunohistochemical Characterization of Pregnancy in $FG^{-/-}$ Mice

The development of the murine placenta in *WT* and $FG^{-/-}$ females was studied in mice at various stages of pregnancy. Several strategies were used in the timed matings of $FG^{-/-}$ females with both *WT* and $FG^{-/-}$ males. $FG^{-/-}$ males breed normally and were used in most cases so that none of embryos would contain Fg. *WT* males were used for special reasons. In these cases, male mice were used that produced β-Gal, the presence of which could then be detected with the chromogenic stain, X-Gal. This strategy was useful in cases in which it became necessary to clearly distinguish maternal from embryonic tissue and cells, particularly in later stages of the abnormal events that occurred *in uteri* with the pregnant $FG^{-/-}$ females.

Embryonic Day 6

Figure 1 illustrates H&E staining of E6.0 embryos from these animals. The embryos of both *WT* and $FG^{-/-}$ mice appear to be at similar stages of development, with giant trophoblasts invading the epithelium and a well-formed ectoplacental cone present (Figure 1, A and B). It is already evident that excessive maternal blood is present in the uterus, in the vicinity of the implantation site, in the $FG^{-/-}$ mouse. The ovaries of both animals examined at this stage exhibit normal architecture and displayed stroma and oocyte development that did not appear to differ in $FG^{-/-}$ and *WT* mice (Figure 1, C and D).

Embryonic Day 7

Figure 2 illustrates the results of a variety of stains that characterize the implantation site of the E7 embryo. The H&E stains show that the ectoplacental cone in the *WT* mouse exhibits signs of the presence of blood (Figure 2A), likely a normal event because of rupturing of capillaries as the cone interdigitates between cells of the decidua and endometrium. This bleeding, which is more pronounced in the $FG^{-/-}$ mouse, likely cannot be effectively controlled in the absence of Fg (Figure 2B). Figure 2C shows the presence of sites of anti-fibrin(ogen) staining that originate from maternal vessels, which are beginning to form at E7. This protein, which serves to limit this bleeding, is present in the ectoplacental cone, in the surrounding decidua and endometrium, and in embryonic distal regions. The presence of Fg and/or fibrin is also noted at the implantation site (Figure 2C). Obviously, no anti-fibrin(ogen) staining is observed in the $FG^{-/-}$ control animal (Figure 2D). Intense anti-FN immunostaining is found in both abembryonic and distal embryonic locations, as well as at the implantation sites in both genotypes (Figure 2, E and F). Profuse interstitial staining for FN is seen in the nondecidualized endometrium, with more focal areas in the decidua. Embryonic endoderm and mesoderm membranes also show the presence of FN. In both genotypes, the VWF immunostains (Figure 2, G and H) show profuse endothelial cell-lined vessels in the ectoplacental cone and implantation site, likely the result of maternal-fetal communication. The distal areas of the embryo also show strong vascularity. Both genotypes also display similar anti-laminin immunostaining throughout the decidua and endometrium, as well as in the embryo itself. Figure 2, I and J, shows that FXIII is co-localized at the implantation site with Fg and FN in the *WT* animal, and with FN in the $FG^{-/-}$ mouse, making this protein available for cross-linking reactions at this site. Similarly, FXIII is also co-localized with these same proteins in the distal embryonic region.

Embryonic Day 8.0

The E8.0 embryos presented in Figure 3, derived from a mating of a Gtrosa male with a $FG^{-/-}$ female, were first whole-mount stained for β-Gal expression. Additional H&E staining of the E8.0 *WT* placenta (Figure 3A) shows a defined implantation of the ectoplacental cone. The fact that embryonic material can be distinguished from maternal tissue in this complex biological environment using this novel approach, because of β-Gal staining solely by embryonic tissue, greatly assists in deriving conclusions regarding the development of the embryonic and maternal placentas.

The sinuses in the E8.0 ectoplacental cone contain maternal blood, and both genotypes are similar in this regard. However, there seems to be a larger amount of blood seepage in the $FG^{-/-}$ mouse (Figure 3B). The implantation site in the *WT* animal stained positively for Fg/fibrin (Figure 3C), FN (Figure 3E), and FXIII (Figure 3I). Although the fibrinoid layer is formed in the $FG^{-/-}$ E8.0 placenta, it obviously does not contain Fg/fibrin (Figure 3D). However, FN (Figure 3F) and FXIII (Figure 3J) are present in this altered fibrinoid layer. In both cases, anti-VWF immunostaining reveals a heavily vascularized implantation region, with endothelium-derived vessels and laminin present throughout the decidua and embryo (Figure 3, G and H).

Figure 2. The murine E7.0 placenta (original magnifications, ×100). **A** and **B:** H&E staining of the *WT* egg cylinder containing an embryo. Mild bleeding is observed in the ectoplacental cone (EC) region (**A**) that is more pronounced in a similarly stained section of a $FG^{-/-}$ female (**B**, **unlabeled arrows**). Bleeding is seen in the egg cylinder cavity of the $FG^{-/-}$ mouse and is also observed in the anti-mesometrial decidual (DE) areas in **A** and **B**. The primitive streak (PS) is also indicated in **A**. **C:** Anti-Fg/fibrin immunostaining shows Fg (or fibrin) (reddish-brown) at the sites of the blood pools in a *WT* mouse. This is obviously not present in a $FG^{-/-}$ mouse (**D**). Fg/fibrin staining is also located around the embryonic endoderm in **C**, as well as at the EC, the implantation site (IS), DE, and endometrium (EM). **E** and **F:** Anti-FN immunostaining shows that this protein is also located throughout the EC, as well as at the embryonic region distal to the IS region and the IS itself, demonstrating that trabecular processes are occurring. Some staining occurs in the DE that is pronounced at the IS. FN is heavily stained throughout the endometrium in both *WT* (**E**) and $FG^{-/-}$ (**F**) mice. **G** and **H:** Double immunostaining of VWF (brown) and laminin (gray) on *WT* (**G**) and $FG^{-/-}$ (**H**) mice tissues. The anti-VWF staining shows numerous endothelial cell-lined vessels in the DE, the EC, the embryonic distal areas, and at the IS of both genotypes. Laminin is also present throughout the DE and EM. The amniotic (AC) and ectoplacental cavities (EPC) are indicated. **I** and **J:** Anti-FXIII immunostaining of *WT* (**I**) and $FG^{-/-}$ (**J**) tissue sections reveals the presence of this protein lining outer membrane regions of the embryos. FXIII appears to be localized around Fg and FN in the implantation site in the *WT* mouse (**I**), and with FN in the $FG^{-/-}$ mouse (**J**).

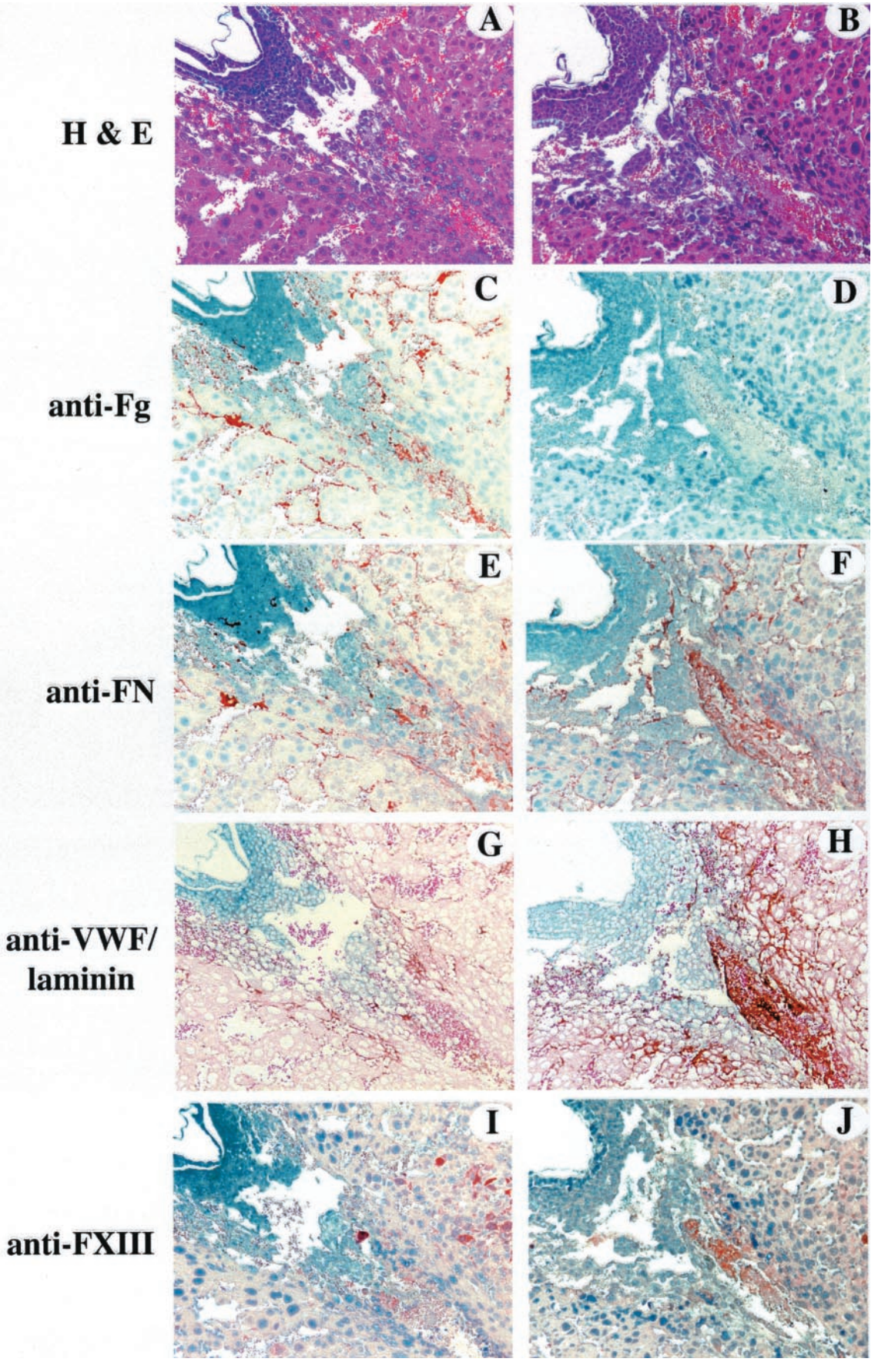
H & E
A
B
anti-Fg
C
D
anti-FN
E
F
anti-VWF/
laminin
G
H
anti-FXIII
I
J

Embryonic Day 9.0

At E9, continued development of the labyrinthine layer occurs in the *WT* placenta, as seen in all panels of Figure 4, and the placenta appears smaller in the $FG^{-/-}$ mouse. A distinct fibrinoid layer is present in the *WT* mouse, surrounding the trophoblast giant cells, and contains Fg/fibrin (Figure 4C), FN (Figure 4E), and FXIII (Figure 4I). Similarly the fibrinoid layer formed in the $FG^{-/-}$ placenta contains FN (Figure 4F) and FXIII (Figure 4J), but not Fg/fibrin (Figure 4D). Signs of separation of the fibrinoid layer are appearing in the $FG^{-/-}$ mouse. As is the case at the earlier gestational ages, the implantation site in both genotypes is heavily vascularized (Figure 4, G and H) with the vessels containing blood and associated blood seepage (Figure 4, A and B).

Embryonic Day 9.75

At E9.75, H&E staining shows that the *WT* chorioallantoic placenta, now fully formed, possesses a clearly defined labyrinth, with an abundance of large blood-filled sinuses where maternal/fetal exchange is occurring, and a spongiotrophoblast layer, separated from the decidua by giant trophoblasts (Figure 5A). Nucleated fetal red blood cells within the labyrinth and nonnucleated maternal red blood cells in the spongiotrophoblast layer and decidua are clearly evident in Figure 5A. Figure 5B shows the presence of a Fg/fibrin-rich fibrinoid layer, with Fg/fibrin surrounding giant cells at the implantation site. The decidua is also heavily stained for interstitial Fg/fibrin. The fibrinoid layer also contains FN (Figure 5C). Anti-VWF staining occurs mainly in the endothelium-derived vessels of the decidua and fibrinoid layer, but not in the labyrinth layer, suggesting that these latter sinuses are not endothelium-derived (Figure 5D). Laminin is present throughout the entire placenta (Figure 5D). Lastly, FXIII is also co-localized at the fibrinoid layer with Fg/fibrin and FN in the *WT* E9.75 placenta (Figure 5E).

A view of the entire egg cylinder of an embryo excised from the uteri of E9.75 *WT* and $FG^{-/-}$ mice, that was initially whole mount stained for β-Gal expression, is shown in Figure 6, with a variety of histochemical and immunohistochemical stainings. In the case of the *WT* female (Figure 6A), a normally developed fetus is present, with the yolk sac-containing embryo-vitelline vessels and blood lakes lining the cylinder. The implantation site is also evident. On the other hand, Figure 6B shows the occurrence of a massive bleeding event in the egg cylinder of a fetus from a $FG^{-/-}$ female. In addition, a much smaller yolk sac and fetus is noted. Examination of the thickened upper wall of the yolk sac cylinder shows the presence of spongiotrophoblasts that most likely originated from a detachment at the implantation site. With use of the Gtrosa male, and the subsequent ability to identify the locations of embryonic tissue, speculation on the position of the original implantation site of this embryo could be made. As can be seen in Figure 6C, embryonic cells in the decidual region of the egg cylinder (top) can be observed (black arrow), and a magnified view of this area (Figure 6D) shows the existence of embryonic giant cells within this region (red arrows). This indicates that detachment of the yolk sac likely occurred from this placental region. Similarly, this latter site also contained overexpression of FN (Figure 6E, black arrows), along with giant cells (Figure 6F, red arrows). VWF (Figure 6, G and H, black arrow), is also present at that site, probably originating from both endothelium-derived vasculature and from platelets present at the site of bleeding. FXIII, along with giant trophoblasts, are also evident at this implantation region, co-localized with FN (Figure 6, I and J).

Rescue of Pregnancies of $FG^{-/-}$ Mice

Using the Fg dosage schedule described in Figure 7, we found that none of the treated female $FG^{-/-}$ mice showed obvious genital bleeding during pregnancy. These mice delivered normally and appropriately managed their offspring. Matings ($n = 5$) of $FG^{-/-}$ males with $FG^{-/-}$ females provided full-term $FG^{-/-}$ litters, ranging from 6 to 11 $FG^{-/-}$ offspring, with both genders represented in nearly equal numbers. Only two of the pups presented fatal neonatal bleeding. The remainder of the pups survived weaning (3 weeks postnatal), and beyond. After weaning the pups, plasma levels of the mothers ($n = 4$) and representative weanlings ($n = 6$) were obtained and did not show detectable levels of plasma Fg. One of the $FG^{-/-}$ mothers experienced three pregnancies after weaning each litter, and, with the same course of Fg treatment, experienced delivery of a total of 18 $FG^{-/-}$ pups.

During the course of the pregnancies, Fg levels in the $FG^{-/-}$ mother were monitored after administration of 10 mg of Fg ($n = 8$). At a time of 24 hours after injection at E4.5 ($n = 8$), Fg levels in $FG^{-/-}$ animals were $\sim 183 \pm 32$ mg/dl (Figure 7A). The following day (E6.5), without ad-

Figure 3. The murine E8.0 placenta (original magnifications, ×100). These embryos were whole-mount stained with X-Gal before sectioning. Embryonic tissue is thus stained a bluish-green. In some cases, eg, H&E staining, this embryonic coloration is not visible because it is overtaken by other stains. **A** and **B:** H&E stainings of *WT* and $FG^{-/-}$ pregnant dams, emphasizing the ectoplacental cone and implantation site regions in the developing chorioallantoic placenta, show blood-containing sinuses and vessels in these regions in both genotypes, with some associated bleeding events outside of the yolk sac cavity that occur in both *WT* and $FG^{-/-}$ mice. **C:** The implantation site, as well as regions of the decidua, stained positively for Fg/fibrin (reddish-brown) in the *WT* mouse, likely from maternal vessels, but obviously not in the $FG^{-/-}$ animal (**D**). **E** and **F:** FN immunostaining (reddish-brown) is co-localized with Fg in the *WT* mouse placenta (**E**) and is present at the implantation site and in stromal regions of the decidua in the $FG^{-/-}$ mouse placenta (**F**). The embryo also contains some FN staining at this gestational age. **G** and **H:** VWF immunostaining (reddish-brown) indicates the presence of endothelial cell-lined vessels in the ectoplacental cone and implantation site regions of both genotypes. These vessels are the likely vehicle of transit of maternal Fg and FXIII found at these sites. The increased levels of VWF at the fibrinoid layer in the $FG^{-/-}$ mouse (**H**) probably arise from platelets that aggregate to attempt to stop bleeding. Laminin (gray, but slightly discolored by the counterstain) stains heavily throughout the decidua and embryo. **I** and **J:** Anti-FXIII immunostaining (reddish-brown) showed the presence of this protein co-localized with Fg and FN in the *WT* mouse, and with FN in the $FG^{-/-}$ mouse. Staining is also observed in stromal regions of the decidua.

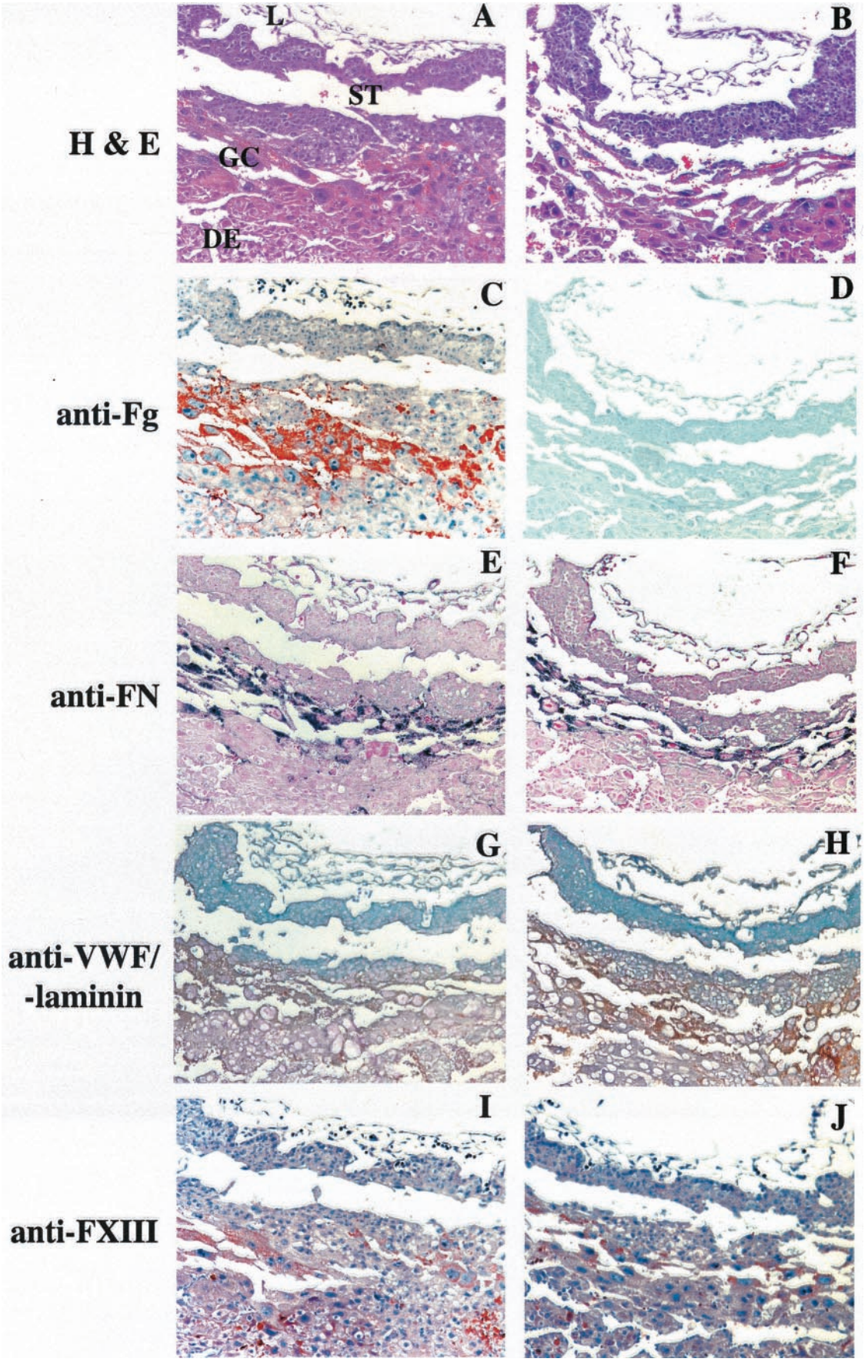
H & E
anti-Fg
anti-FN
anti-VWF/
-laminin
anti-FXIII
L
A
ST
GC
DE
B
C
D
E
F
G
H
I
J

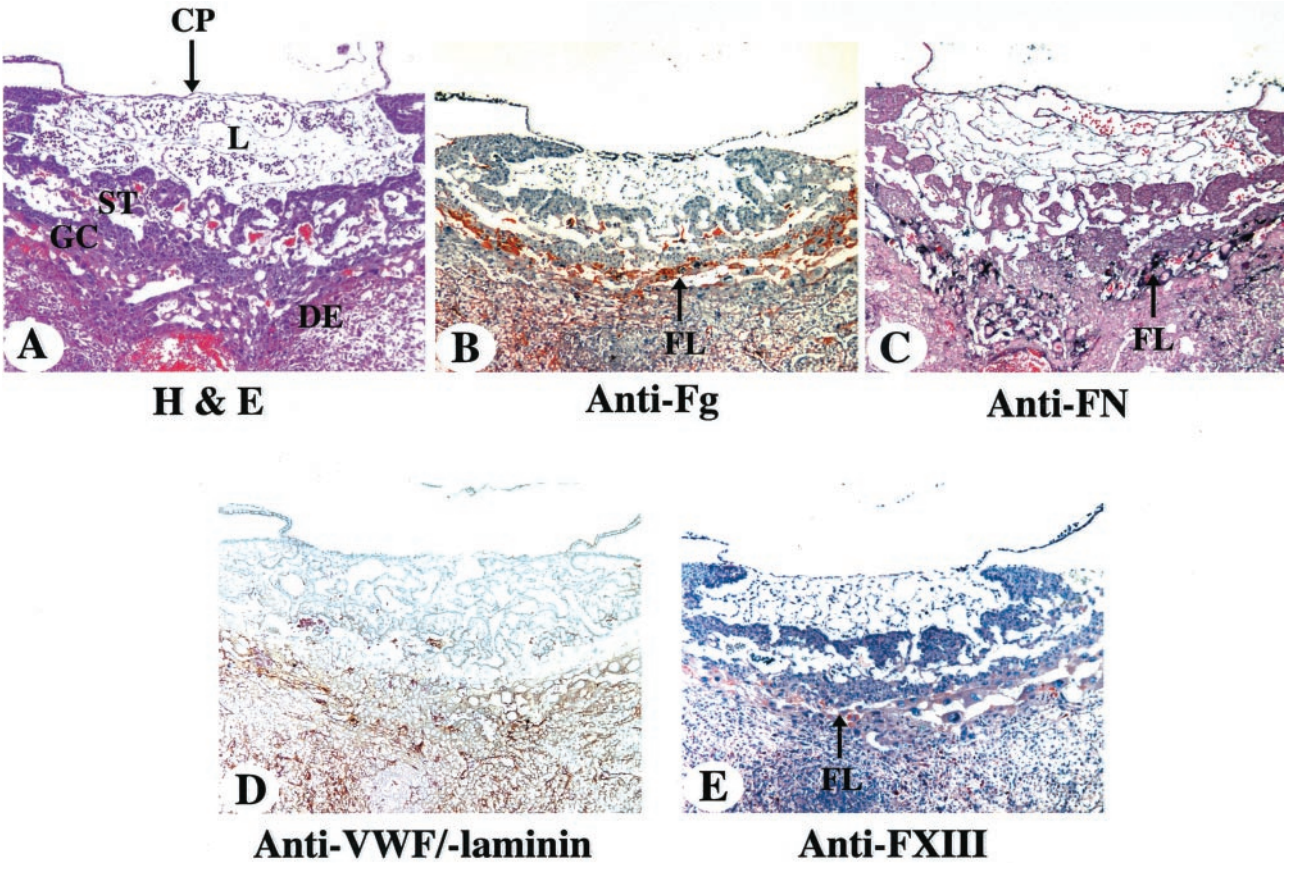

Figure 5. The murine *WT* E9.75 placenta (original magnifications, ×100). **A:** H&E staining of *WT* sections illustrating the fusion of the maternal decidua (DE) with the embryonic layers in the *WT* placenta. The labyrinth (L) layer, which is fused to the spongiotrophoblast (ST) layer, followed into the DE by the giant cell (GC) layer, is clearly observed, as is the chorionic plate (CP). **B:** Anti-Fg/fibrin immunostaining (reddish-brown) of serial sections of this tissue indicates the presence of the Fg/fibrin-containing fibrinoid layer (FL), and staining throughout the DE. **C:** Anti-FN immunostaining (gray/black) indicates the co-localization of this protein with Fg/fibrin in the FL. **D:** Anti-VWF immunostaining (reddish-brown) demonstrates that endothelial cell-lined vessels are present in the maternal and embryonic regions of the placenta. Anti-VWF staining is also co-localized with that of Fg/fibrin and FN. Laminin (gray) is present throughout the labyrinth and decidual regions. **E:** Anti-FXIII immunostaining (reddish-brown) shows the presence of this protein in the FL and its co-localization with Fg/fibrin and FN.

ditional treatment, Fg levels were ~77 ± 22 mg/dl (normal levels in *WT* nonpregnant female mice are, ~185 mg/dl), and the protein was below the level of detection (20 mg/dl) 3 days after injection (Figure 7A). Injections of 10 mg of Fg were subsequently made at E8.5, and every 2 days afterward, up to E18.5. In all cases, Fg levels of ~70 mg/dl to 140 mg/dl were found on the day after injection, with the lower ranges obtained in late pregnancy, possibly indicating increased consumption at times approaching delivery. In all cases, at times of 2 days after Fg treatment, very low levels of Fg (20 mg/dl to 30 mg/dl) were found in plasma of the pregnant $FG^{-/-}$ mice.

A time course of Fg determinations on *WT* (n = 8) and $FG^{+/-}$ (n = 14 to 16) pregnant females, without any additional Fg administration, demonstrated that Fg levels rose slightly from their normal values after E8.5 during the course of pregnancy (Figure 7B), whereas the value for $FG^{+/-}$ pregnant females remained somewhat constant. In this study, we find that initial levels of Fg as low as 90 mg/dl could support normal pregnancy without intervention (Figure 7B). This is also the case in the few humans that have been studied in this regard.[24,25] Of course, it is possible that even lower concentrations of this protein would suffice.

As a result of this information, a number of Fg administration protocols were attempted, and we found that a minimal dosage schedule of 10 mg of Fg at E8.5 and E17.5 would result in a successful vaginal deliveries in $FG^{-/-}$ females.

Figure 4. The murine E.9.0 placenta (original magnifications, ×200). **A** and **B:** H&E staining of *WT* and $FG^{-/-}$ embryos shows the attachment of the labyrinth (L) to spongiotrophoblasts (ST) in the *WT* tissue (**A**). The giant cell (GC) layer is also observable at the interface between the decidua (DE) and ST layers. **B:** The placenta in the $FG^{-/-}$ mouse appears smaller than its *WT* counterpart, and the ST layers are beginning to separate from the DE. **C** and **D:** Anti-Fg/fibrin (reddish-brown) immunostaining clearly shows a Fg/fibrin-rich fibrinoid layer between the GC and ST layers (**C**). None of this staining is seen the $FG^{-/-}$ mouse tissue (**D**). **E** and **F:** Anti-FN staining (gray-black) is co-localized with Fg/fibrin in the fibrinoid layer in the *WT* (**E**) and $FG^{-/-}$ (**F**) placentas. **G** and **H:** Anti-VWF staining (reddish-brown) demonstrates the presence of endothelial cell-lined vessels in the fibrinoid layer and DE of both the *WT* (**G**) and $FG^{-/-}$ (**H**) tissue sections, that are likely supplying the maternal circulation to the embryo. Very little staining is observed in the labyrinth, suggesting that the large sinuses present therein are not derived from the endothelium. Anti-laminin staining (gray) of the same tissue shows the presence of laminin throughout the ST, L, and DE layers in both genotypes. **I** and **J:** Anti-FXIII immunostaining (reddish-brown) demonstrates the presence of FXIII in the interfacial fibrinoid layer of both genotypes, as well in stromal regions of the DE.

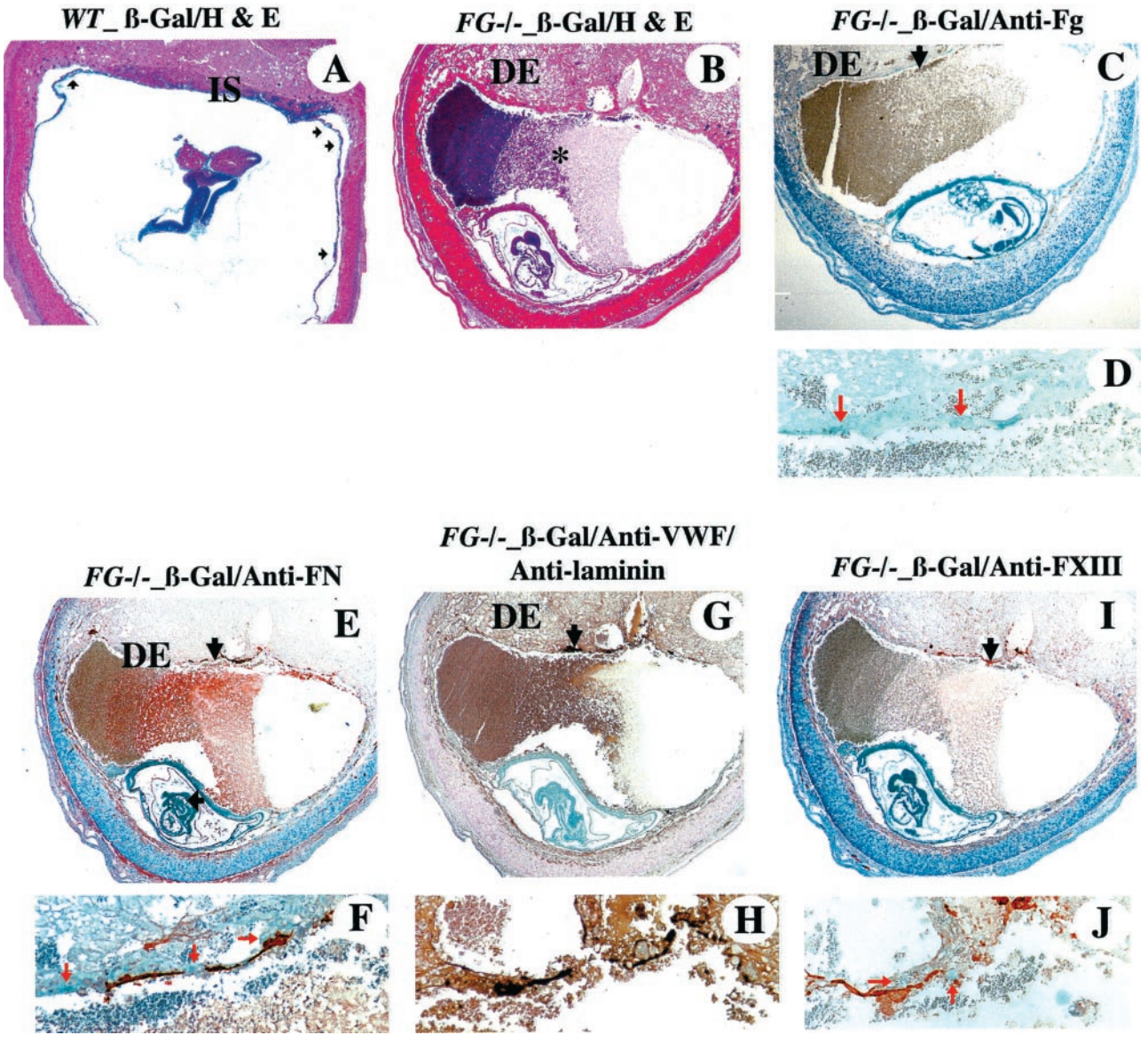

Figure 6. The murine E9.75 egg cylinders of pregnant *WT* and $FG^{-/-}$ mice (original magnifications, ×40). These samples were whole-mount stained with X-Gal before sectioning. **A:** H&E staining of the E9.75 *WT* mouse egg cylinder shows a normally developing embryo with its yolk sac (YS) lining the cylinder wall. YS vasculature and blood lakes are seen (**black arrows**). The uterine implantation site (IS) in the decidua (DE) is indicated. H&E (**B**) and anti-Fg/fibrin (**C**) stainings of the $FG^{-/-}$ E9.75 egg cylinder illustrate a massive bleeding event (**asterisk**) in the egg cylinder cavity. The presence of embryonic cells (**filled arrow**) in a DE site that is remote from the position of the fetus (**C**) indicates that placental detachment likely has occurred from this site (the implantation site). An expanded view of the area in the vicinity of the **black arrow** shows the presence of embryonic giant cells (**red arrows**) in this same region. **E:** Anti-FN staining shows the presence of FN in the same region of the DE (**filled arrow**) as the embryonic cells in **C**. GC (**red arrows**, **inset**) associated with the FN layer are clearly seen in an expanded view (**F**) of a region of the **black arrow** in **E**. This further suggests that this area was the original implantation site. **G:** Anti-VWF/anti-laminin and FXIII stainings show numerous endothelial cell-lined vessels and perhaps platelets (**arrow**), which is observed more clearly in an expanded view of the implantation site (**H**). **I:** Anti-FXIII immunostaining demonstrates co-localization of this protein with Fg/fibrin, FN, and VWF at the implantation site. **J:** An expanded view of the **arrowed** region of **I** shows embryonic giant cells (**red arrows**) around the FXIII immunostains. Original magnifications, ×40 (**A–C**, **E**, **G**, and **I**); **D**, **F**, **H**, and **J** were arbitrarily expanded for purposes of ease of visualization.

Characteristics of the E9.75 Chorioallantoic Placenta of a $FG^{-/-}$ Pregnant Mouse Administered Fg

Figure 8 presents representations of the embryos and implantation sites of an E.9.75 $FG^{-/-}$ pregnant female (mated with a Gtrosa male) who had been administered Fg. The final dose of Fg was provided at E8.5, and the plasma level of Fg of this mouse at sacrifice (E9.75) was 102 mg/dl (see Figure 7A). Photographs of the embryo egg cylinders *in utero* are shown in Figure 8 for E9.75 $FG^{-/-}$ (Figure 8A) and *WT* (Figure 8B) mice, as well as a $FG^{-/-}$ gravida administered Fg (Figure 8C). The severe intrauterine bleeding observed in the $FG^{-/-}$ animal (Figure 8A) was not observed in the rescued $FG^{-/-}$ mouse (Figure 8C), which had the same gross features as the *WT* mouse uterus at this same gestational stage (Figure 8B). The microscopic features of the implantation of one of the embryos in panel C also appear to be normal. Specifically, H&E stainings of an embryo attached to the

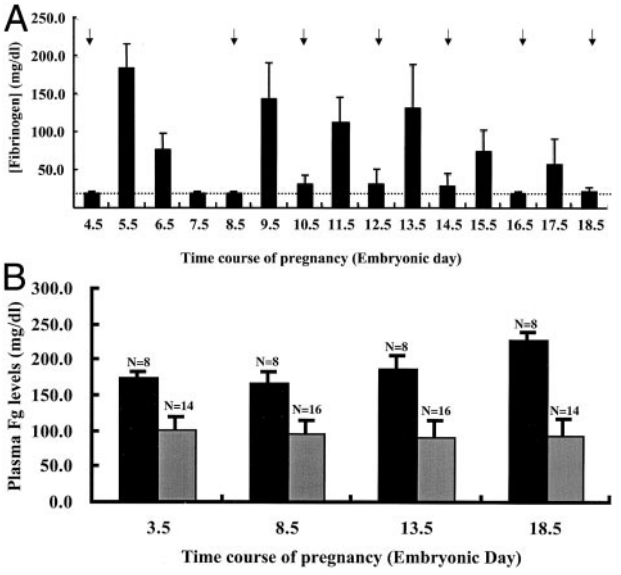

Figure 7. Plasma levels of Fg during pregnancies of various genotypes. **A:** The consumption of exogenous Fg by pregnant $FG^{-/-}$ mice. A quantity of 10 mg of Fg was injected into pregnant females at E4.5 and blood drawn for 3 consecutive days. Other injections of the same quantity were made every second day (**arrows**) and Fg levels determined. The **dotted vertical line** represents the lowest level of Fg detection in our assay. **B:** The Fg concentration in plasmas of *WT* (**black bars**) and heterozygous ($FG^{+/-}$) pregnant mice (**gray bars**) during the course of pregnancy. Plasma was taken by eye bleedings from individual *WT* mice ($n = 8$) and $FG^{+/-}$ mice ($n = 14$ to 16). Fg levels were determined at E3.5, E8.5, E13.5, and E18.5.

uterus of panel C (Figure 8D) show well-defined labyrinth and spongiotrophoblast layers, one or both containing large sinuses, lacunae, and arteries, with fetal and maternal blood present. The spongiotrophoblast layer is clearly separated from the decidua by a layer of fetal trophoblast giant cells. A clear distinction of maternal- and embryonic-derived tissue can be made from the β-Gal stainings (blue) of serial sections of an embryo of panel C, shown in panels E, F, H, and I (Figure 8). The only possible source of the Fg immunostaining present throughout the maternal decidua (Figure 8E) is from that injected into the plasma of the mother. This maternal Fg is also observed in random vessels of the spongiotrophoblast layer (Figure 8E), showing that vascular communication between the mother and fetus has been established. A heavier layer of Fg/fibrin, along with FN (Figure 8F) and FXIII (Figure 8H), appears at the interfacial implantation site that composes the fibrinoid layer anchoring the trophoblast giant cells. FN and FXIII also appear similarly within spongiotrophoblast-located vessels, indicating these two proteins may have interacted in the circulation. The strong immunostaining for FN in interstitial regions of the labyrinth, chorionic plate, yolk sac, decidua, and the fact that Fg and FXIII are not co-localized with interstitial FN in the embryonic labyrinth and chorionic plate, suggests that this form of FN may be fetally derived, whereas Fg/fibrin and FXIII at the fibrinoid layer may need to originate from maternal circulation. The labyrinth, spongiotrophoblast, yolk sac, and decidua of this same placenta are heavily vascularized with embryonic and maternal endothelium-derived cells, as evidenced by the positive VWF immunostaining of Figure 8G. Finally, a ×40 view of the β-Gal/FN doubly-stained embryo attached to the uterine wall (a lower resolution view of Figure 8F) is presented in Figure 8I. Contrasting this rescued pregnancy at E.9.75 with the unrescued pregnancy of Figure 6B, shows the clear benefits that result from Fg administration. The bleeding and placental detachment observed in the unrescued animal are not observed in the mouse treated with Fg, and the rescued mouse seems to maintain the same egg cylinder-uterine contact as is present in the same stage *WT* mouse (Figure 6A).

Discussion

Genetic alterations that lead to predispositions to bleeding are associated with clinical complications during pregnancy. The most vivid example of this is in congenital afibrinogenemia, which results in genital bleeding and spontaneous miscarriage in the first 6 to 8 weeks of pregnancy.[18–20] From a total five deliveries in four women, three cesarean deliveries have been reported with Fg replacement therapy,[24–26] and two vaginal deliveries were experienced with similar treatment.[26,27] We found the same general situation to exist in our mouse model of a total Fg deficiency. In cases of pregnancies of $FG^{-/-}$ mice, obvious genital bleeding was observed at any time between E7 to E9, and miscarriage occurred before E10. These pregnancies were rescued by administration of Fg, and normal vaginal deliveries occurred. Without Fg replacement therapy, the $FG^{-/-}$ mother did not survive because of the heavy bleeding that accompanied the miscarriage. This indicates that the Fg required for maintenance of the pregnancy can be solely supplied by maternal plasma.

This murine model of congenital afibrinogenemia thus seems to be very suitable to investigate mechanistic features of spontaneous miscarriage in humans with this genetic defect, and, even more important, to define the role of Fg in supporting a successful outcome of pregnancy.

The histochemical and immunohistochemical assessment of embryonic, placental, and decidual tissues in timed pregnancies allowed precise determination of the course of fetal and maternal demise in Fg-deficient pregnant mice. The first subtle event, visualized in the uteri of pregnant animals on E6, is an exacerbation of the normal bleeding that occurs in regions surrounding the ectoplacental cone. Lack of Fg allows for continued bleeding, leading to lacunae filled with blood at E8 to E9 of the gestational period. Blood seepage from the sinuses of the developing labyrinths of the placenta are more extensive in $FG^{-/-}$ mice. The bleeding continues throughout the placental development, so that by E9 large areas of bleeding initiate the disruption of the placenta and yolk sac from the endometrium, causing complete placental abruption on E9.75. As a result, the pregnant mice die from profuse bleeding. The Fg deficiency does not alter embryonic development, but formation of the placenta and yolk sac is significantly compromised. Both the placentas and yolk sacs in afibrinogenemic animals are

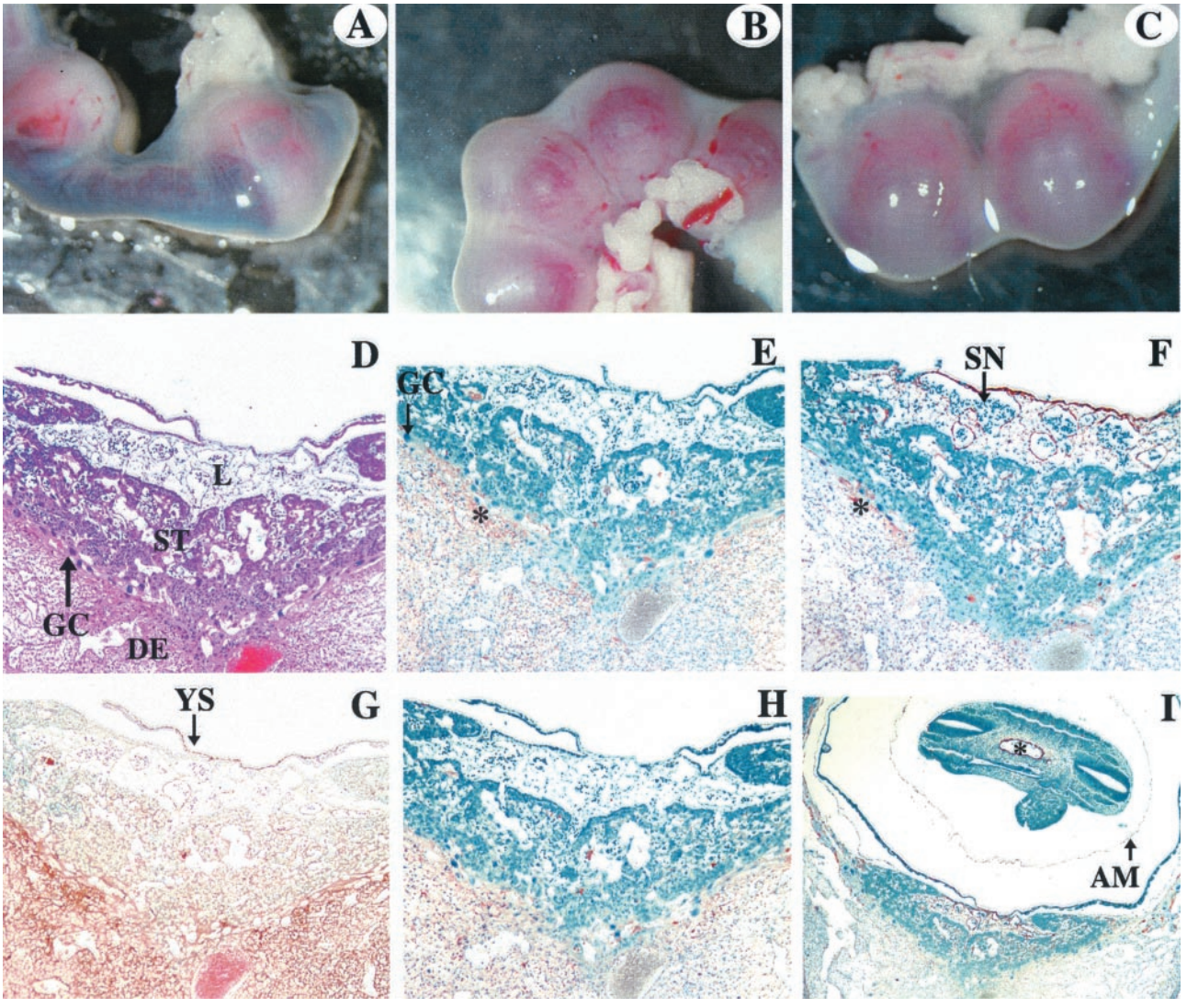

Figure 8. Rescue of pregnancies in E.9.75 $FG^{-/-}$ pregnant mice as a result of Fg administration. Gross examinations of E9.75 uteri containing embryos within their egg cylinders show severe intrauterine bleeding in the $FG^{-/-}$ mouse (**A**), as compared to a *WT* mouse (**B**). **C:** The egg cylinders of E9.75 $FG^{-/-}$ mouse that was administered Fg possessed the gross features as the *WT* embryos and egg cylinders. **D:** H&E stain (original magnification, ×100) of the placenta and implantation site (IS) of a rescued E9.75 $FG^{-/-}$ mouse embryo shows a normal labyrinth (L) layer, with embryonic blood in large sinuses attached to the yolk sac (YS). A spongiotrophoblast (ST)-containing area is present, with an interfacial layer of giant cells (GC) between the ST and decidual (DE) regions. A large blood-filled maternal artery is observed in the DE. **E:** Anti-Fg/fibrin (reddish-brown) staining (original magnification, ×100) of a serial section of **D** of the tissue of the treated $FG^{-/-}$ mouse, showing that Fg that was administered to plasma of the $FG^{-/-}$ mother is present in vessels within the DE, as well as in the fibrinoid layer (FL) at the IS (**asterisk**). Randomized staining is also present in the vessels in the embryonic (blue-green) ST area, but is not visible in the vessels of the labyrinthine region. **F:** Anti-FN (reddish-brown) staining (original magnification, ×100) shows the presence of FN surrounding macrophages in the DE layer and some ST cells of the Fg-treated $FG^{-/-}$ mother. This protein is abundant in the labyrinth, especially around the large sinuses (SN), as well as in the chorionic plate, and co-localizes with Fg/fibrin at the FL at the IS (**asterisk**). **G:** Anti-VWF (reddish-brown)/anti-laminin (gray) staining (original magnification, ×100) illustrates the endothelial cell-lined vessels of the maternal DE, and the embryonic ST, labyrinth, and YS areas of the treated E9.75 $FG^{-/-}$ mouse. **H:** Anti-FXIII (reddish-brown) staining (original magnification, ×100) shows abundant FXIII immunostaining in the DE area, including the FL. **I:** A ×40 view of the anti-FN (reddish-brown)-stained tissue section (**F**). FN staining in the treated $FG^{-/-}$ mouse is also noted, lining the dorsal aorta of the embryo (**asterisk**), as well as the amnion (AM). The now well-vascularized YS fully lines the cylinder cavity, and is clearly attached to the IS. Embryos used in **D** to **H** were whole-mount stained with X-Gal before sectioning.

smaller than those found in corresponding *WT* animals. A most important site of Fg/fibrin deposition is the fibrinoid layer that starts to peel from the decidua in the absence of Fg/fibrin. This event is associated with disruption of sinusoids of the labyrinths. This leads to severe hemorrhage along the planes of placental-decidual attachment. This adherence is enforced by other proteins including laminin, FN, and FXIII, which co-localize with Fg in *WT* mice. A lack of Fg does not change this typical distribution pattern, but its presence is required to give sufficient stability to the placental-decidual binding.

Platelet adhesion and aggregation at the site of vascular compromise are the first key events that serve to arrest bleeding.[28,29] By virtue of bridging GPIIb/IIIa on adjacent platelets, Fg leads to platelet aggregation, which ultimately forms a platelet thrombus. VWF contributes to the activation of the integrin, $\alpha IIb\beta 3$, on the platelets through an inside-out signaling pathway.[30] The lack

of Fg does not seem to alter the distribution of VWF on the extensive vascular network, which develops both within the embryo and placenta as well as the surrounding decidua. In the absence of Fg, it is thought that VWF contributes to platelet adhesion and aggregation.[31] Even in the absence of both Fg and VWF, platelet thrombi can form in mice that lack both VWF and Fg, although adhesion and aggregation is delayed.[31] This finding shows that the abnormal bleeding in the uteri of $FG^{-/-}$ mice is not because of a compromise in platelet aggregation or formation of platelet thrombus. Rather, the profuse bleeding in these animals is likely caused by the coagulation defect that results from lack of Fg. This protein is thought to be critical to coagulation because the insoluble fibrin matrix stabilizes the thrombus.[2] In $FG^{-/-}$ mice, the thrombi that are formed are quite unstable and lead to vessel embolization and occlusion.[31] The weakest point of thrombi in $FG^{-/-}$ mice seems to lie at the thrombus-vessel wall interface.[31] This event is likely to play a role in exacerbation of the placental abruption in the $FG^{-/-}$ mice. The ability to easily form thrombi is thought to be shared by humans with a Fg deficiency, because blood from these patients also forms thrombi on subendothelium in perfusion chambers.[32] This thrombotic tendency in afibrinogenemic patients seems to be an additional factor in the development of complications of pregnancy.

Hypercoagulable responses resulting from a number of mutations that lead to thrombosis of the uteroplacental vessels, spiral artery vasculopathies, and impaired placental perfusion are all associated with abnormal development of the fetus, pregnancy losses, and obstetrical complications. Notable among these are genetic predispositions toward thrombophilia, such as the FV-Leiden mutation,[33] leading to thrombosis because of anti-coagulant protein C resistance; the homozygous methylenetetrahydrofolate mutation,[33] resulting in hyperhomocysteinemia and a consequent thrombotic condition; the prothrombin G20210A mutation,[34] resulting in elevated plasma prothrombin concentrations and the associated risks of coagulopathies; and the vascular thrombotic dispositions of an anti-phospholipid syndrome.[35] Many of the early associations between thrombophilia and pregnancy loss were studied through retrospective analyses with small numbers of patients, thus tempering the conclusion as to whether causal relationships exist between complications of pregnancy and thrombosis. However, more recent case-controlled prospective studies support the view that genetic markers of thrombophilia may predispose women to a number of severe complications during pregnancy.[34,36,37]

In the E8 mouse, the chorioallantoic placenta is developing, and abnormalities appear in the pregnancy of the $FG^{-/-}$ female. The spongiotrophoblast layer is beginning to separate and shows signs of hypoplasia. This leads to further separation, which is evident in the E9.0 embryos. In this case, a smaller placenta in the $FG^{-/-}$ mouse is seen, with a spongiotrophoblast layer that has begun to detach from the fibrinoid layer. At E9.75, terminal events in the pregnancy have occurred in the $FG^{-/-}$ mouse. Massive bleeding is seen in the egg cylinder cavity and an apparently forceful detachment of the spongiotrophoblast layer from the fibrinoid layer is observed, with portions of the giant cell-associated fibrinoid layer remaining at the implantation site and cells from the spongiotrophoblast layer present in the detached yolk sac. These events are sufficient to terminate the pregnancy, in that clear placental abruption has occurred.

The results of this investigation reveal very important elements of pregnancies in normal mice and divulge a possible encompassing role for Fg in this process. It seems as though the course of pregnancy and development of the placenta in mice possess some similar features to that of humans. These include formation of a fibrinoid layer that contains Fg, FN, laminin, and FXIII. Fg is a critical component of the fibrinoid layer and stable attachment of the spongiotrophoblast to this layer does not occur in afibrinogenemic mothers. Placental abruption in these animals thus involves separation of the fibrinoid layer from the spongiotrophoblast layer, and this is another novel finding that resulted from this study.

Thus, the role of Fg in supporting a successful pregnancy certainly involves its function as a hemostatic agent, by assuring that normal bleeding during development of immature vessels is effectively controlled. In addition, Fg is required in a less appreciated role, by assisting in formation of a stable fibrinoid layer that is essential for anchoring the spongiotrophoblast layer to the decidua. This process may involve the interaction of stromal FN, itself bound to collagen at the surface of decidual cells at the implantation site,[38] with its integrin receptors, eg, $\alpha_5\beta_1$, on invading spongiotrophoblast cells.[39] Stromal Fg, supplied by the vasculature of the mother, may also bind to FN and/or the $\alpha_5\beta_1$ integrin,[40] stabilizing the fibrinoid layer. FXIII, which is supplied by maternal plasma and by macrophage-derived mononuclear cells in the decidua, is capable of further stabilizing the fibrinoid layer via crosslinking of FN to Fg[41,42] and of FN to decidua-derived collagen.[43]

In conclusion, the loss of embryo in afibrinogenemic mice is because of an abortive process that is initiated as an exacerbation of the hemorrhage that normally occurs around E6 during the critical stage of maternal-fetal vascular development and at a time when the embryo is invading the maternal decidua. This event gives rise to a robust bleeding that does not cease during days 8 and 9 of gestation. Ultimately, the profuse bleeding causes extensive placental disruption that results in the loss of embryo and death of the mother. This entire course of events can be normalized by elevation of the maternal plasma Fg levels and successful vaginal deliveries experienced. This shows that embryonically derived Fg is not required for a completion of a successful pregnancy and that all Fg needed in this regard is derived from the mother.

Acknowledgments

We thank Dr. Siamak Tabibzadeh for reading and providing helpful commentary on this article; and Ms. Stacey Raje, Ms. Angeliek Andersen, and Ms. Nichole Haughee for their management of the animal colony.

References

1. Kant JA, Fornace Jr AJ, Saxe D, Simon MI, McBride OW, Crabtree GR: Evolution and organization of the fibrinogen locus on chromosome 4: gene duplication accompanied by transposition and inversion. Proc Natl Acad Sci USA 1985, 82:2344–2348
2. Doolittle RF: Fibrinogen and fibrin. Annu Rev Biochem 1984, 53:195–229
3. McRitchie DI, Girotti MJ, Glynn MF, Goldberg JM, Rotstein OD: Effect of systemic fibrinogen depletion on intraabdominal abscess formation. J Lab Clin Med 1991, 118:48–55
4. Kuijper PH, Gallardo-Torres HI, Lammers JW, Sixma JJ, Koenderman L, Zwaginga JJ: Platelet and fibrin deposition at the damaged vessel wall: cooperative substrates for neutrophil adhesion under flow conditions. Blood 1997, 89:166–175
5. Martin P: Wound healing—aiming for perfect skin regeneration. Science 1997, 276:75–81
6. Gartner TK, Ogilvie ML: Peptides and monoclonal antibodies which bind to platelet glycoproteins IIb and/or IIIa inhibit clot retraction. Thromb Res 1988, 49:43–53
7. Costantini V, Zacharski LR: The role of fibrin in tumor metastasis. Cancer Metastasis Rev 1992, 11:283–290
8. Lassila R, Peltonen S, Lepantalo M, Saarinen O, Kauhanen P, Manninen V: Severity of peripheral atherosclerosis is associated with fibrinogen and degradation of cross-linked fibrin. Arterioscler Thromb 1993, 13:1738–1742
9. Rabe F, Solomen E: Uber faserstoffmangel im blut bei einem falle von haemophilic. Dtsch Arch Klin Med 1920, 132:240–245
10. Martinez J: Congenital dysfibrinogenemia. Curr Opin Hematol 1997, 4:357–365
11. Neerman-Arbez M, Honsberger A, Antonarakis SE, Morris MA: Deletion of the fibrogen alpha-chain gene (FGA) causes congenital afibrogenemia. J Clin Invest 1999, 103:215–218
12. Neerman-Arbez M, de Moerloose P, Bridel C, Honsberger A, Schonborner A, Rossier C, Peerlinck K, Claeyssens S, Di Michele D, d'Oiron R, Dreyfus M, Laubriat-Bianchin M, Dieval J, Antonarakis SE, Morris MA: Mutations in the fibrinogen Aα gene account for the majority of cases of congenital afibrinogenemia. Blood 2000, 96:149–152
13. Duga S, Asselta R, Santagostino E, Zeinali S, Simonic T, Malcovati M, Mannucci PM, Tenchini ML: Missense mutations in the human beta fibrinogen gene cause congenital afibrinogenemia by impairing fibrinogen secretion. Blood 2000, 95:1336–1341
14. Asselta R, Duga S, Simonic T, Malcovati M, Santagostino E, Giangrande PLF, Mannucci PM, Tenchini ML: Afibrinogenemia: first identification of a splicing mutation in the fibrinogen gamma chain gene leading to a major gamma chain truncation. Blood 2000, 96:2496–2500
15. Margaglione M, Santacroce R, Colaizzo D, Seripa D, Vecchione G, Lupone MR, De Lucia D, Fortina P, Grandone E, Perricone C, Di Minno G: A G-to-A mutation in IVS-3 of the human gamma fibrinogen gene causing afibrinogenemia due to abnormal RNA splicing. Blood 2000, 96:2501–2505
16. Neerman-Arbez M, de Moerloose P, Honsberger A, Parlier G, Arnuti B, Biron C, Borg JY, Eber S, Meili E, Peter-Salonen K, Ripoll L, Vervel C, d'Oiron R, Staeger P, Antonarakis SE, Morris MA: Molecular analysis of the fibrinogen gene cluster in 16 patients with congenital afibrinogenemia: novel truncating mutations in the FGA and FGG genes. Hum Genet 2001, 108:237–240
17. al-Mondhiry H, Ehmann WC: Congenital afibrinogenemia. Am J Hematol 1994, 49:343–347
18. Dube B, Agarwal SP, Gupta MM, Chawla SC: Congenital deficiency of fibrinogen in two sisters. A clinical and haematological study. Acta Haematol 1970, 43:120–127
19. Matsuno K, Mori K, Amikawa H: A case of congenital afibrinogenemia with abortion, intracranial hemorrhage and peritonitis. Jpn J Clin Haematol 1977, 98:722–724
20. Evron S, Anteby SO, Brzezinsky A, Samueloff A, Eldor A: Congenital afibrinogenemia and recurrent early abortion: a case report. Eur J Obstet Gynecol Reprod Biol 1985, 19:307–311
21. Asahina T, Kobayashi T, Okada Y, Itoh M, Yamashita M, Inamato Y, Terao T: Studies on the role of adhesive proteins in maintaining pregnancy. Horm Res 1998, 50:37–45
22. Ploplis VA, Wilberding J, McLennan L, Liang Z, Cornelissen I, DeFord ME, Rosen ED, Castellino FJ: A total fibrinogen deficiency is compatible with the development of pulmonary fibrosis in mice. Am J Pathol 2000, 157:703–708
23. Suh TT, Holmback K, Jensen NJ, Daugherty CC, Small K, Simon DI, Potter S, Degen JL: Resolution of spontaneous bleeding events but failure of pregnancy in fibrinogen-deficient mice. Genes Dev 1995, 9:2020–2033
24. Inamoto Y, Terao T: First report of case of congenital afibrinogenemia with successful delivery. Am J Obstet Gynecol 1985, 153:803–804
25. Kobayashi T, Asahina T, Maehara K, Itoh M, Kanayama N, Terao T: Congenital afibrinogenemia with successful delivery. Gynecol Obstet Invest 1996, 42:66–69
26. Kobayashi T, Kanayama N, Tokunaga N, Asahina T, Terao T: Prenatal and peripartum management of congenital afibrinogenaemia. Br J Haematol 2000, 109:364–366
27. Trehan AK, Fergusson IL: Congenital afibrinogenaemia and successful pregnancy outcome. Case report. Br J Obstet Gynaecol 1991, 98:722–724
28. Kloczewiak M, Timmons S, Hawiger J: Localization of a site interacting with human platelet receptor on carboxy-terminal segment of human fibrinogen gamma chain. Biochem Biophys Res Commun 1982, 107:181–187
29. Farrell DH, Thiagarajan P: Binding of recombinant fibrinogen mutants to platelets. J Biol Chem 1994, 269:226–231
30. Shattil SJ, Kashiwagi H, Pampori N: Integrin signaling: the platelet paradigm. Blood 1998, 91:2645–2657
31. Ni H, Denis CV, Subbarao S, Degen JL, Sato TN, Hynes RO, Wagner DD: Persistence of platelet thrombus formation in arterioles of mice lacking both von Willebrand factor and fibrinogen. J Clin Invest 2000, 106:385–392
32. Weiss HJ, Turitto VT, Vicic WJ, Baumgartner HR: Fibrin formation, fibrinopeptide A release, and platelet thrombus dimensions on subendothelium exposed to flowing native blood: greater in factor XII and XI than in factor VIII and IX deficiency. Blood 1984, 63:1004–1014
33. Grandone E, Margaglione M, Colaizzo D, Cappucci G, Paladini D, Martinelli P, Montanaro S, Pavone G, Di Minno G: Factor V Leiden, C > T MTHFR polymorphism and genetic susceptibility to preeclampsia. Thromb Haemost 1997, 77:1052–1054
34. De Groot CJ, Bloemenkamp KW, Duvekot EJ, Helmerhorst FM, Bertina RM, Van Der Meer F, De Ronde H, Oei SG, Kanhai HH, Rosendaal FR: Preeclampsia and genetic risk factors for thrombosis: a case-control study. Am J Obstet Gynecol 1999, 181:975–980
35. Gharavi AE, Pierangeli SS, Levy RA, Harris EN: Mechanisms of pregnancy loss in antiphospholipid syndrome. Clin Obstet Gynecol 2001, 44:11–19
36. Kupferminc MJ, Eldor A, Steinman N, Many A, Bar-Am A, Jaffa A, Fait G, Lessing JB: Increased frequency of genetic thrombophilia in women with complications of pregnancy. N Engl J Med 1999, 340:9–13
37. Martinelli I, Taioli E, Cetin I, Marinoni A, Gerosa S, Villa MV, Bozzo M, Mannucci PM: Mutations in coagulation factors in women with unexplained late fetal loss. N Engl J Med 2000, 343:1015–1018
38. Wewer UM, Faber M, Liotta LA, Albrechtsen R: Immunochemical and ultrastructural assessment of the nature of the pericellular basement membrane of human decidual cells. Lab Invest 1985, 53:624–633
39. Damsky CH, Fitzgerald ML, Fisher SJ: Distribution patterns of extracellular matrix components and adhesion receptors are intricately modulated during first trimester cytotrophoblast differentiation along the invasive pathway, in vivo. J Clin Invest 1992, 89:10–22
40. Suehiro K, Mizuguchi J, Nishiyama K, Iwanaga S, Farrell DH, Ohtaki S: Fibrinogen binds to integrin alpha(5)beta(1) via the carboxyl-terminal RGD site of the A alpha-chain. J Biochem (Tokyo) 2000, 128:705–710
41. Procyk R, Adamson L, Block M, Blomback B: Factor XIII catalyzed formation of fibrinogen-fibronectin oligomers—a thiol enhanced process. Thromb Res 1985, 40:833–852
42. Procyk R, Blomback B: Factor XIII-induced crosslinking in solutions of fibrinogen and fibronectin. Biochim Biophys Acta 1988, 967:304–313
43. Paye M, Lapiere CM: The lack of attachment of transformed embryonic lung epithelial cells to collagen I is corrected by fibronectin and FXIII. J Cell Sci 1986, 86:95–107